

## Summary Description of Selected Projects in the Jin group

### **Solar Energy Related Technologies R&D in the Jin Lab**

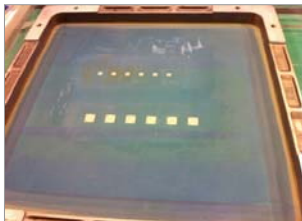
1. Dye sensitized solar cells (FTO-glass-free, low cost solar cells)
2. Low cost Si slicing
3. Thermoelectric materials
4. Compliant thermal interface material (TIM)
5. Self-cleaning glass surface
6. Concentrated solar power (CSP) solar thermal generator coatings
7. Ultra-high-density vertical solar cell array

### **Improved Dye Sensitized Solar Cells**

- Conversion efficiency of ~9-10% obtained in DSSC solar cells using home-made and screen-printed anatase TiO<sub>2</sub> nanoparticle anodes. ( $J_{sc} \sim 17 \text{ mA/cm}^2$ ,  $V_{oc} \sim 0.78 \text{ V}$ , and fill factor of ~0.7 are obtained).
- For scale-up fabrication toward larger size DSSCs, various filler approaches are being investigated, e.g., using high-aspect-ratio TiO<sub>2</sub> nanotubes or double-wall carbon nanotube additions to improve charge transport and reduce microcracking. 3 x 3cm size cells have been demonstrated, with larger cells being constructed.
- FTO-glass-free DSSC solar cells are being developed as the use of FTO glass can amount to ~40% of the DSSC cost, and also the IR drop by the FTO is severe and makes it difficult to scale-up toward large area solar cell panel due (unless many ~1 cm wide stripe subcells are stitched).

### **Screen printed DSSC**

Screen



Support for FTO glass substrate



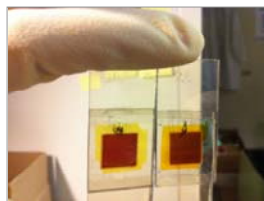
Paste being screened



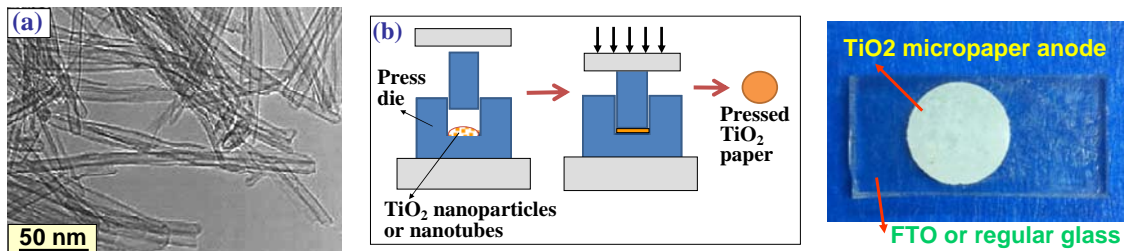
Paste on anode FTO glass



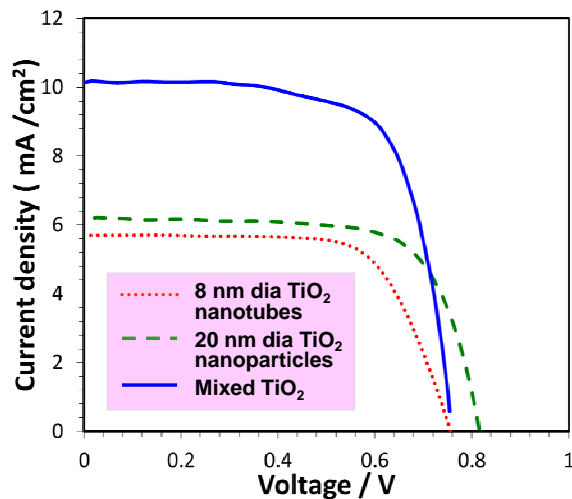
DSSC cells



## New DSSC anodes with TiO<sub>2</sub> micropaper approach



8 nm dia, 2  $\mu\text{m}$  long TiO<sub>2</sub> nanotubes (hydrothermally synthesized) mixed with 20 nm diameter TiO<sub>2</sub> nanoparticles (1:2 volume ratio) and press-compacted for free-standing DSSC solar cell anodes.

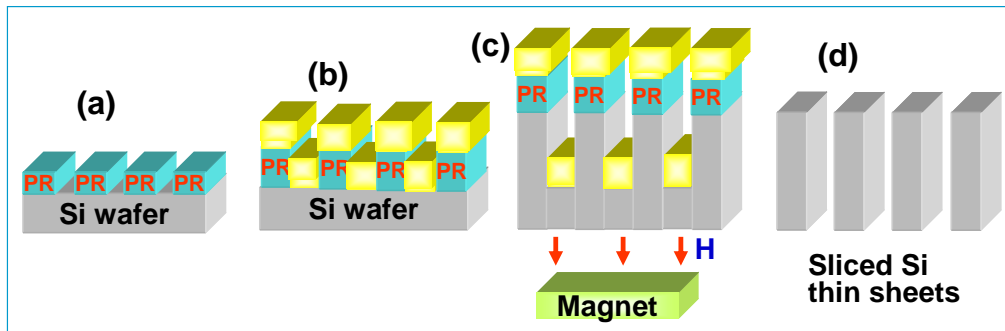


Current density vs voltage relationship (J-V curves) of the DSSC solar cells with different types of TiO<sub>2</sub> micropapers. (1:2 mix of nanoparticles and nanotubes produces DSSC solar cell efficiency of ~6% or higher).

## Si Nano/Micro-Shaping for Reduced Cost Photovoltaic Solar Cells

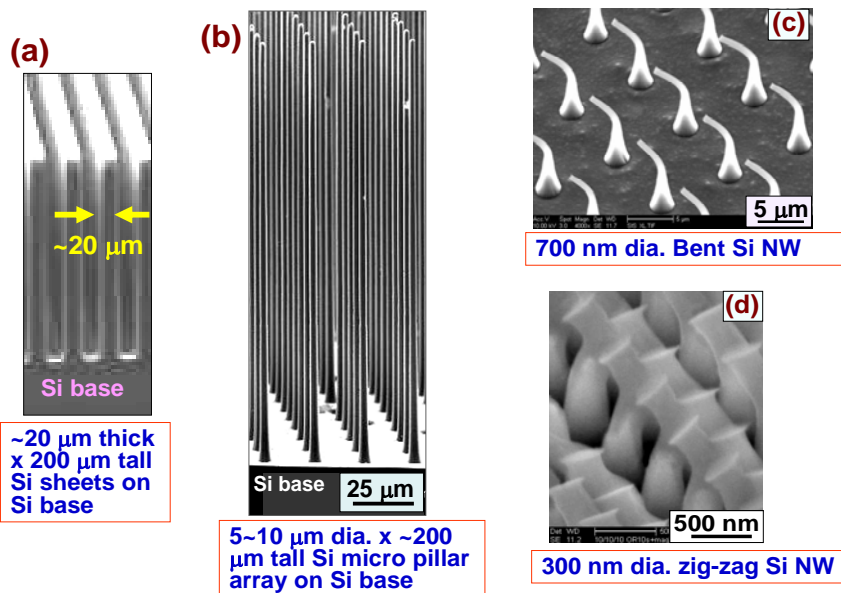
### **Massively parallel, Si chemical slicing for low cost, low-loss thin wafers**

- Current PV solar cells are too expensive for wide applications as renewable energy source.
- One of the major cost factors is the Si material, which amounts to almost one-half of the single crystal solar cell cost.
- Typical wire-saw slicing of Si wafer results in ~200  $\mu\text{m}$  loss of Si per cut for ~200  $\mu\text{m}$  thick wafer slicing.
- We have developed a new slicing technique that reduces the cut loss to as little as ~10  $\mu\text{m}$ , which also allows a fabrication of very thin Si wafers (~5-30  $\mu\text{m}$  thick) for additional reduction in Si materials usage in PV solar cells.
- This novel technique can also be utilized for shaping of Si into tall nano-micro wires, zig-zag nanowire arrays, nano-tunnels, very thin flexible wafers for various applications such as energy, photonics, electronics, biomedical devices as well as flexible circuits.



Schematics of the magnetically direction-guided, catalytic silicon slicing process. (a) Photoresist line pattern on Si ingot surface using photolithography, (b) Magnetic catalyst layer deposition (5-20  $\mu\text{m}$  wide and 5-20  $\mu\text{m}$  spaced apart, up to 20,000 parallel etch lines over 20 cm length Si ingot) for massively parallel Si wafer slicing, (c) Magnetic guided electroless etching into Si depth, (d) photoresist lift-off and remaining Au catalyst removal to obtain thin microsheets of sliced Si.

### Thin sliced Si ribbons, pillars, bent nanowires by catalytic shaping

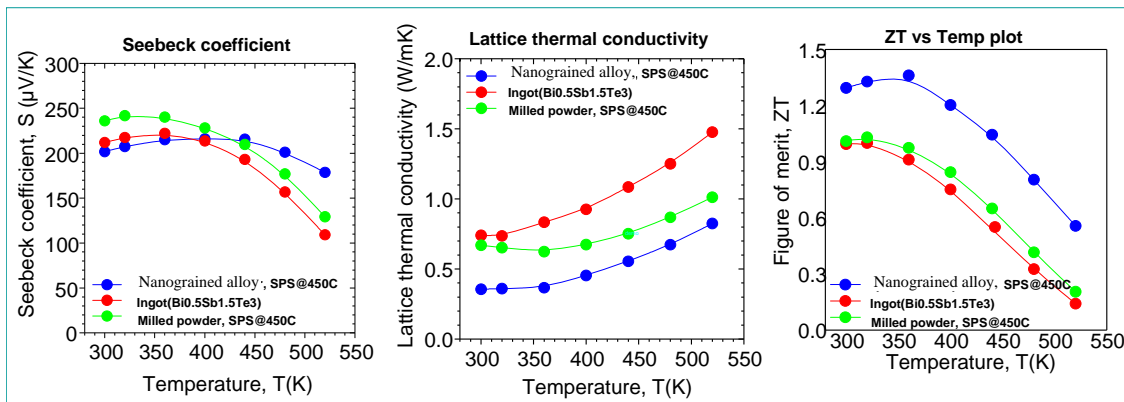
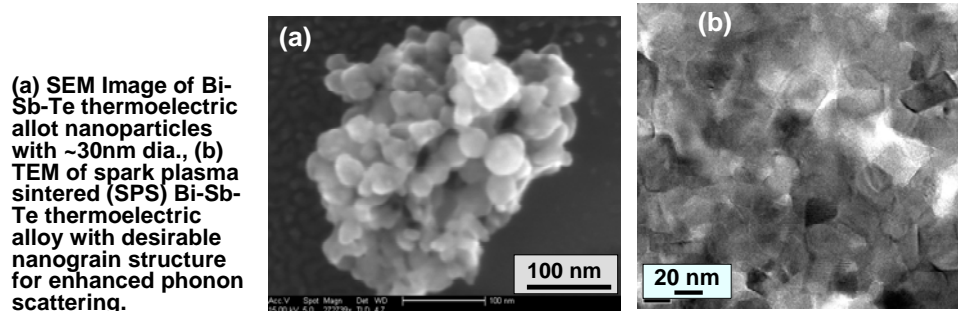


### Thermoelectric Materials

--- The thermoelectric figure of merit ( $ZT$ ) can be expressed as  $ZT = (S^2\sigma/k)T$  (where  $S$  is the Seebeck Coefficient,  $\sigma$  is the electrical conductivity, and  $k$  is the thermal conductivity. For higher  $ZT$ , these materials parameters need to be optimized.

--- Thermoelectric (TE) alloys such as Bi-Sb-Te and skutterudites are promising energy materials for waste heat recovery and solar energy generation. For enhanced TE properties such as the energy conversion efficiency, it is essential to increase the phonon scattering and reduce the thermal conductivity. Various nanoparticle synthesis techniques based on physical, chemical or mechanical approaches are utilized at UCSD to produce

variety of nanoparticles of thermoelectric alloys and sintered nanograined alloys having excellent thermoelectric properties. Further nanostructure controls are being investigated to increase the phonon scattering, Seebeck Coefficient, and electrical conductivity of various thermoelectric materials.



## Self-cleaning glass surface

--- Nanostructured glass or silica surfaces having superhydrophobic and omniphobic properties have been developed for maintenance-free solar panel surface (with minimal needs for washing/cleaning during solar cell use lifetime).

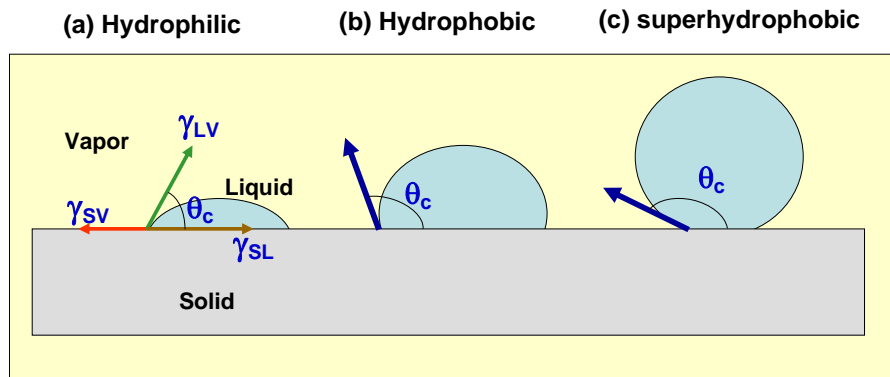
---Wear resistant, superhydrophobic glass surface made of transparent ceramic nanostructure, rather than easily smearable polymer coating, has been produced.

--- For anti-fingerprint surface, both super-hydrophobic + super-oleophobic (=super-omniphobic) characteristics are required for “*Maintenance-free, anti-reflective PV cell arrays*” and for “*Anti-fingerprint, anti-Reflection touch panel surface*” as outdoor air environment as well as human fingerprint excretion material contains both water base and oil base components.

--- Anti-fingerprint surface made of super-omniphobic nano-glass with wear resistance and AR properties has been studied and developed for the past 4 yrs at UCSD.

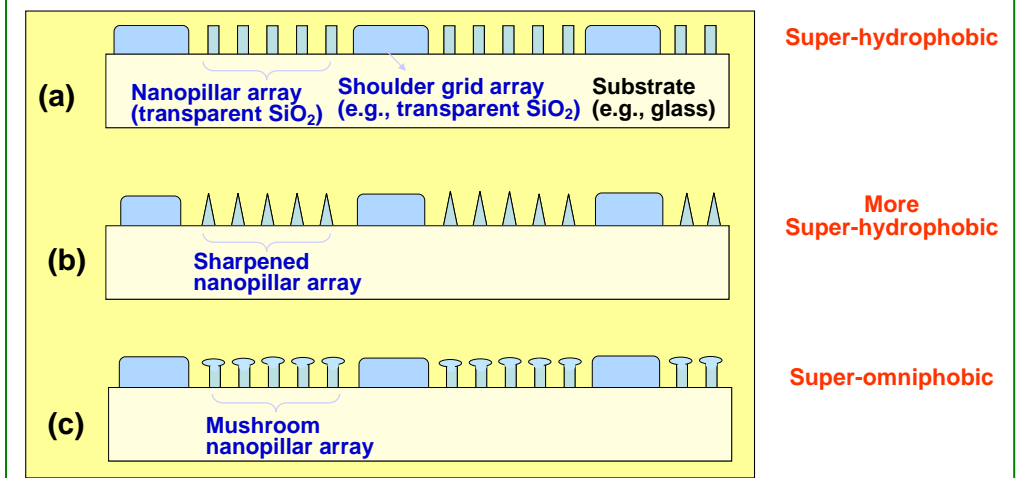
--- Scale-up manufacturability is considered in the nanostructure design.

**Self-Cleaning Surface --- water nonwetting & oil nonwetting are necessary conditions.**

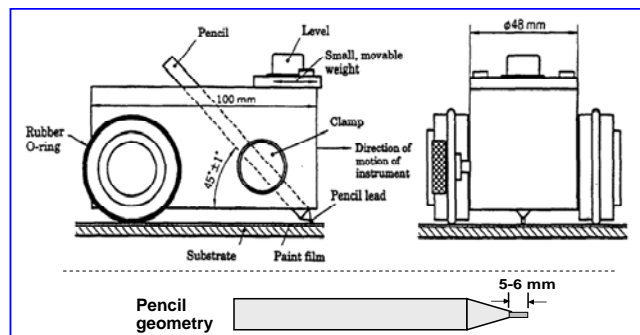


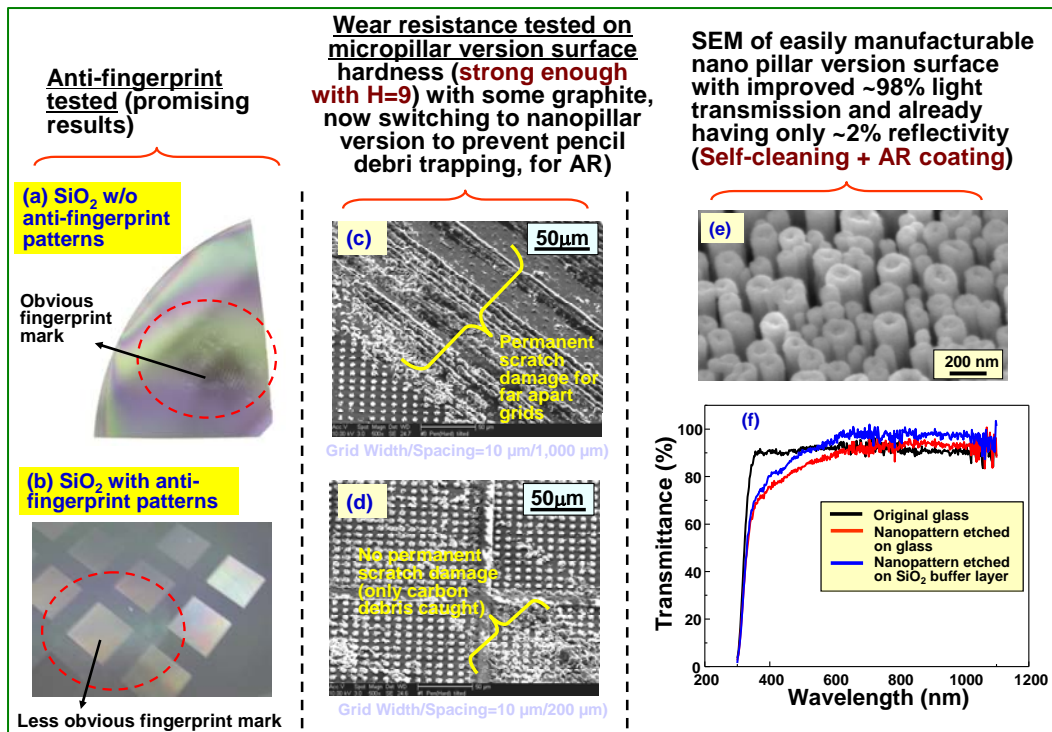
--- Schematic illustration of contact angles for hydrophilic, hydrophobic, and superhydrophobic surfaces. A similar definition of **oleophilic, oleophobic and superoleophobic**, also applies for oil wetting instead of water wetting.  
 --- Super-omniphobic ceramic surface (having both superhydrophobic and superoleophobic) has been demonstrated.

**Composite of nanopillars/nanowires (providing super-omniphobic nonwetting properties) and flat but transparent shoulder grid array (providing non-scratch wear resistance).**



**JIS K 5600 Standard Hardness Tester using 45° Tilted Pencil for scratch testing for evaluation of wear-resistance**



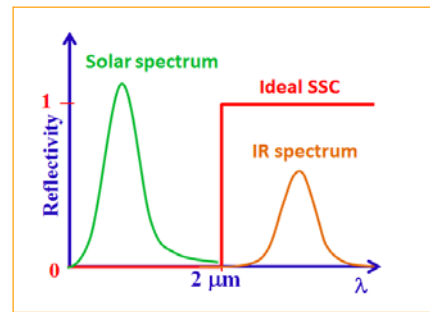


## Concentrating Solar Power --- High Performance Nanostructured Spectrally Selective Coating

- Concentrating solar power (CSP) --- A viable, commercialized technology that competes effectively with the photovoltaic solar energy. This Carnot cycle based energy conversion is based on focusing sunlight onto the Spectrally Selective Coating (SSC) on a steel pipe that contains a molten salt heated by the absorbed thermal energy. The molten salt is sent to the power plant where steam is generated to operate steam turbines and generate electricity. The solar thermal Carnot cycle efficiency is high, ~40% at the current operating temperature of ~450°C. the goal of this DOE-funded project is to further increase the efficiency toward ~60% regime by developing new, more efficient, sunlight absorbing SSC layer that will enable a 700 -750°C CSP operation. These efficiency values are much higher than the typical photovoltaic energy conversion efficiency (~25%).
- Spectrally selective coating (SSC) --- A critical component that enables high-temperature and high-efficiency operation of concentrated solar power (CSP) systems. SSC has a profound impact on the performance and cost of CSP systems. The optical properties of the SSC, namely, absorption in the solar spectrum range (UV/Vis) is maximized by materials design as we pursue a bandgap-adjusted, nanoparticle

semiconductor materials while the reflectance, while the undesirable black body emission loss in IR (infrared) regime is minimized.

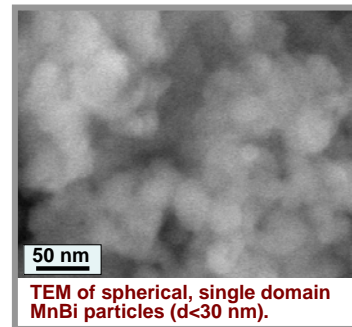
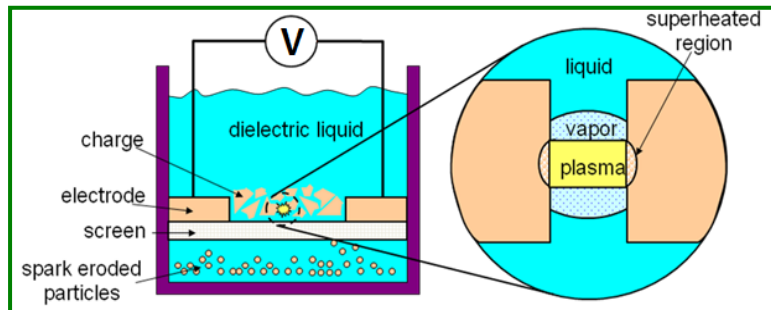
- For higher temperature operation to achieve higher Carnot efficiency, the semiconductor material nanoparticles need to be protected from oxidation, e.g., with the synthesis of a variety of nano core-shell structures. configuration surface layer as investigated in this project.



### Rare-Earth-Free Permanent Magnet Alloys

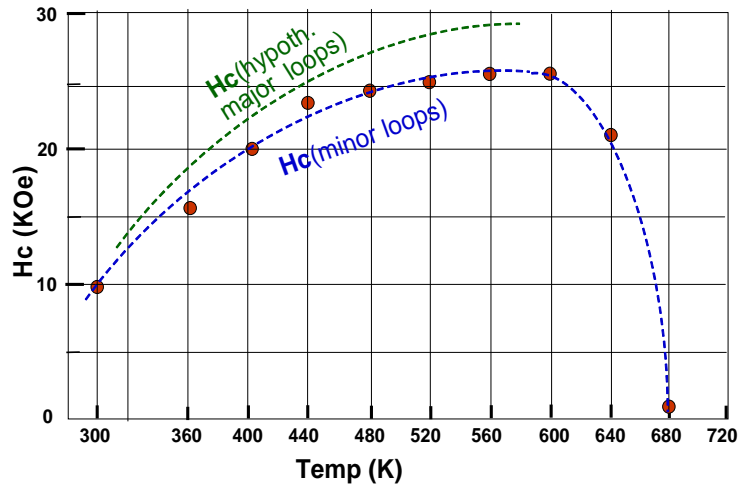
--- The high price of rare earth metals, especially Dy utilized in Nd-Fe-B magnets has instigated active R&D toward new, rare-earth-free permanent magnet materials.

--- We employ a spark erosion technique to easily produce nanoparticles of Mn-Bi magnet alloys so that the high magnetocrystalline anisotropy of the material is fully utilized with minimal domain wall motion. Soft-magnet / hard-magnet exchange coupled spring magnets with higher coercive force are also being developed.



Spark erosion principle for nanoparticle synthesis.

**H<sub>c</sub> vs Temp. for spark eroded MnBi nanoparticles**  
 --- H<sub>c</sub> approaching 30 KOe  
 --- The stability of H<sub>c</sub> well beyond 200°C, up to ~300°C (573K) demonstrated.  
 --- Exchange coupled core-shell magnets being designed.



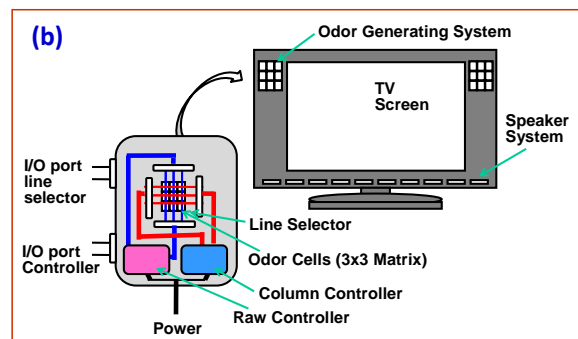
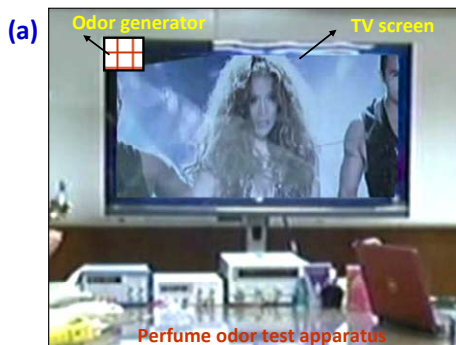
### Smell-O-Vision Devices Using X-Y Matrix Controlled Odor Release

--- Virtual reality can be made more realistic with a three-dimensional or other sensory input. Out of the five senses humans have (i.e., vision, sound, smell, taste and touching), we have already incorporated the first two senses in modern communications and entertainment systems such as TVs, mobile phones, computers, and movies.

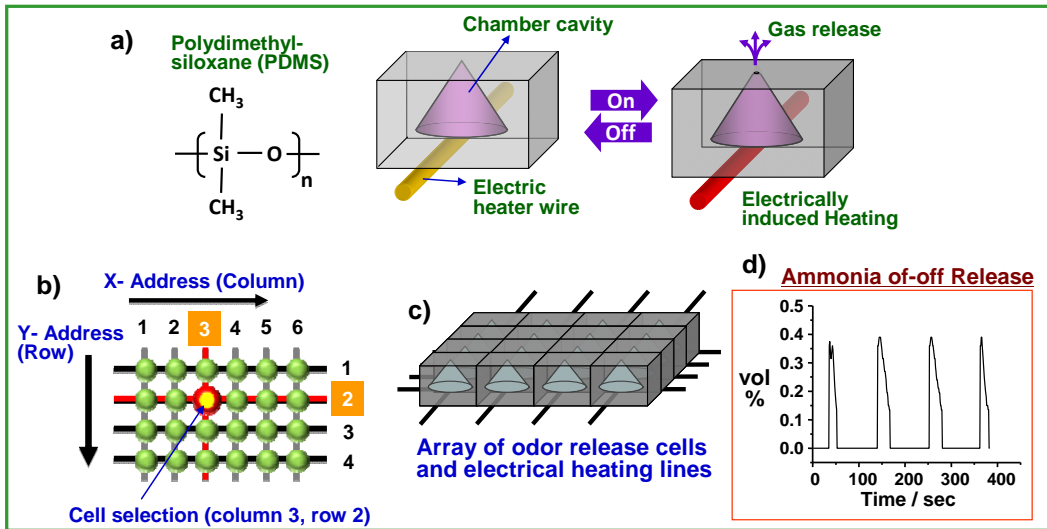
--- To enhance the quality of entertainment and communications, it would be nice to incorporate another sense, a sense of smell. Synchronization of odor release to the corresponding image on the screen can be accomplished conveniently by electronic signals using a reliable, inexpensive, and not cumbersome device.

--- Odor releasing devices that allow easy on-off switching of odor flux could have a significant impact on the effectiveness of virtual reality. We have developed a repeatable new odor/gas releasing system having a novel X–Y matrix addressable capability.

--- Odor generating system with improved kinetics and reliability, test controllability with a system embedded in TV, and demonstrate programmable odor release in a synchronized manner together with the visual images on screen are being investigated.



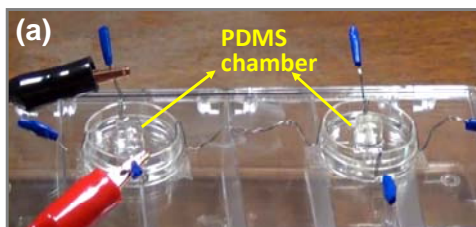
Odor releasing TV (a) Jennifer Lopez TV scene with synchronized release of Jennifer Lopez perfume (“Live by Jennifer Lopez”) smell. (b) Diagram of communication for the operation of hardware.



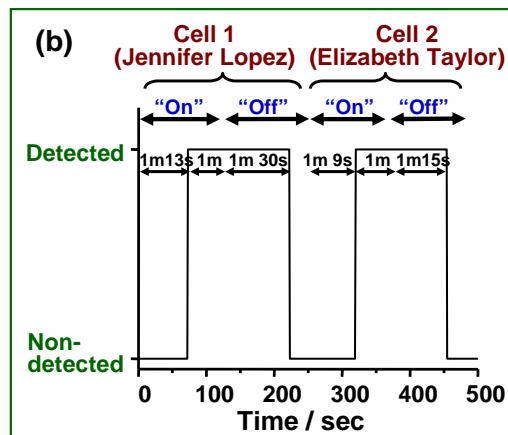
Schematics of the mechanism of gas/odor release device **(a)** PDMS elastic chamber material with heat-activated gas release. **(b)** a diagram illustrating the x-y coordinated cell selection method, which allows chamber opening only when simultaneous X- and Y- heaters are activated for selective cell gas release, **(c)** an example x-y matrix structured odor generating system with 4 by 4 cells, **(d)** example on-off release of a model gas by heater control.



Laboratory demo of X-Y matrix odor release device



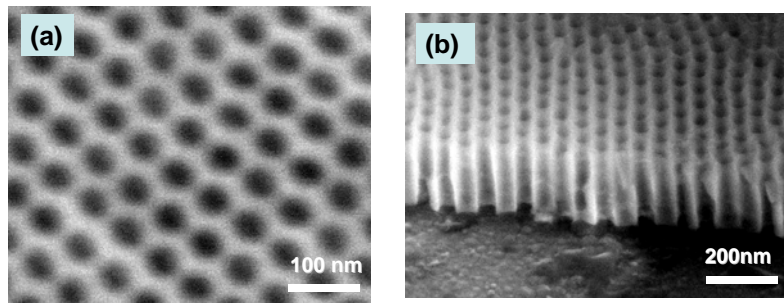
Selective odor generation. **(a)** Experimental set-up, **(b)** Real-time responses of human olfaction measured for the smell of two perfumes, the "Live by Jennifer Lopez" and the "Passion by Elizabeth Taylor".



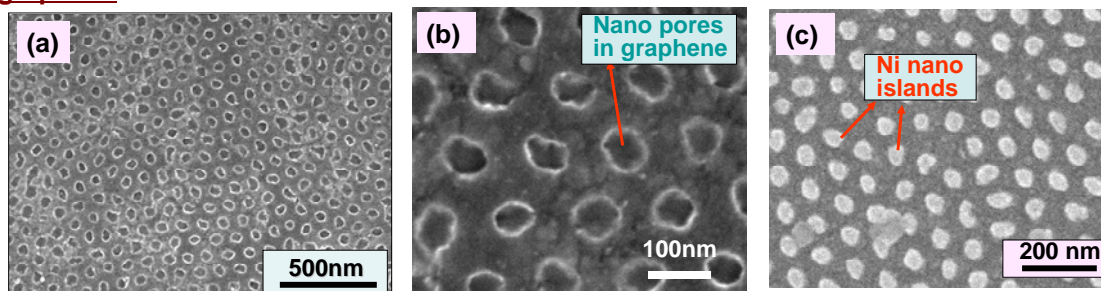
## Graphene Processing and Properties

- Graphene is a very exciting new material with many potential applications. For semiconductor use with graphene's high carrier mobility and other unique properties, the band-gap has to be opened.
- New Anodized Aluminum Oxide (AAO) template with smaller 40-50 nm dia pores, 200-300nm thickness developed.
- Such AAO templates were utilized to pattern graphene layer (CVD grown on Cu substrate followed by removal of Cu). Honeycomb-geometry graphene was obtained so as to produce enhanced edge effect and band-gap opening. Magnetic nano-island arrays are also being fabricated for enhanced magneto-transport properties.
- Electronic and magnetic properties of nano-modified graphene layers are being evaluated.

New AAO template with smaller pores. (a) top, (b) side view



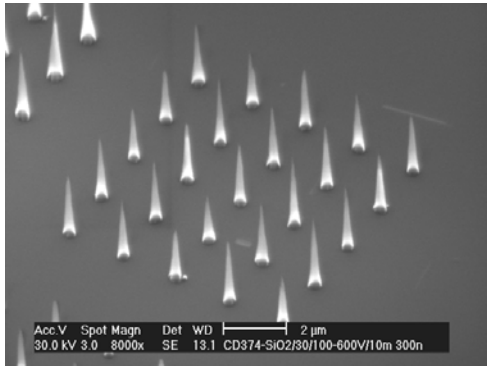
(a),(b) Nano-patterned graphene layer, (c) Ni nano particle attached graphene



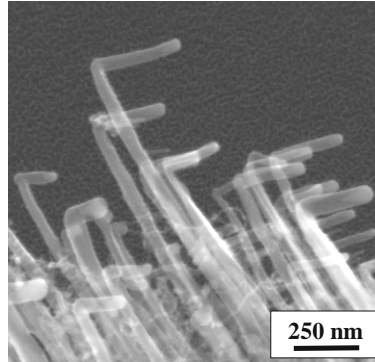
## Carbon Nanotube Geometry Control

- Sharply pointed carbon nanotubes can have even smaller tip diameter because of elimination of catalyst particle radius of curvature. Such sharp tips are advantageous for enhanced field emission, high-resolution metrology, bio-insertion of molecules and functionalities, etc.
- While straight carbon nanotubes are relatively easy to grow, curved or bent nanotubes are difficult to synthesize --- For technical applications, sharply bent or zig-zag carbon nanotubes are important for nano spring applications, sidewall tracing scanning probes, routing of nanoelectronics interconnects, and possible introduction of defects to form hetero-junction nanotube semiconductor devices.

**Periodic and Aligned Carbon Nanotube Array by Electric-Field-Guided CVD Growth**

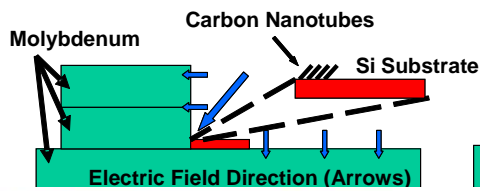


**90 Degree Bent Nanotubes**

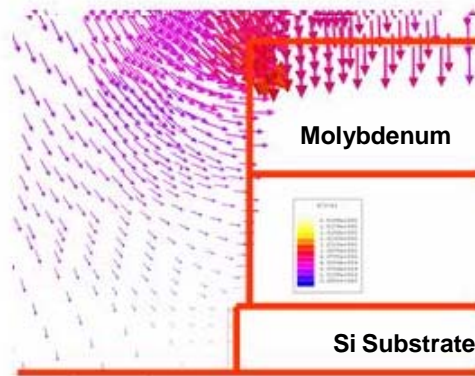
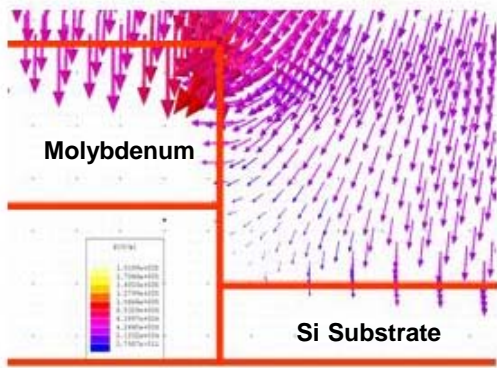
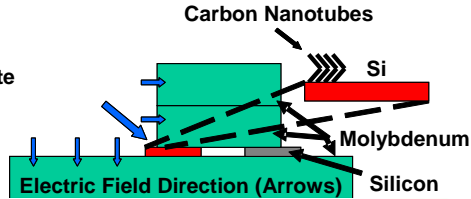


**Bending and orienting of Carbon Nanotubes:  
Experimental Setup and Electric-Field-Direction Modeling**

**First Growth Stage**

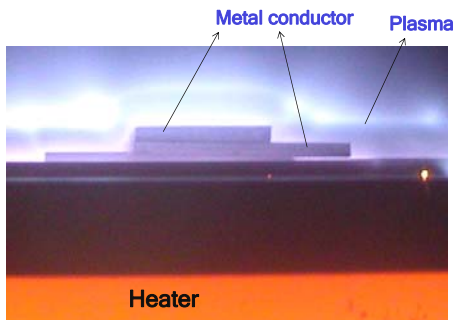


**Second Growth Stage**

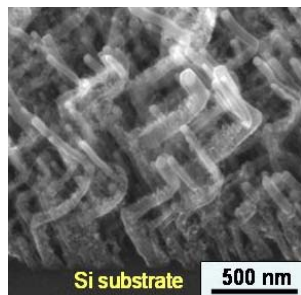


*E vector modeling done using Maxwell SV*

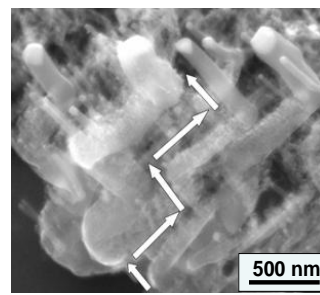
**CVD growth chamber for bent or zig-zag nanotube growth**



**Three Step Zig-Zag Structure**



**Five Step Zig-Zag Structure**



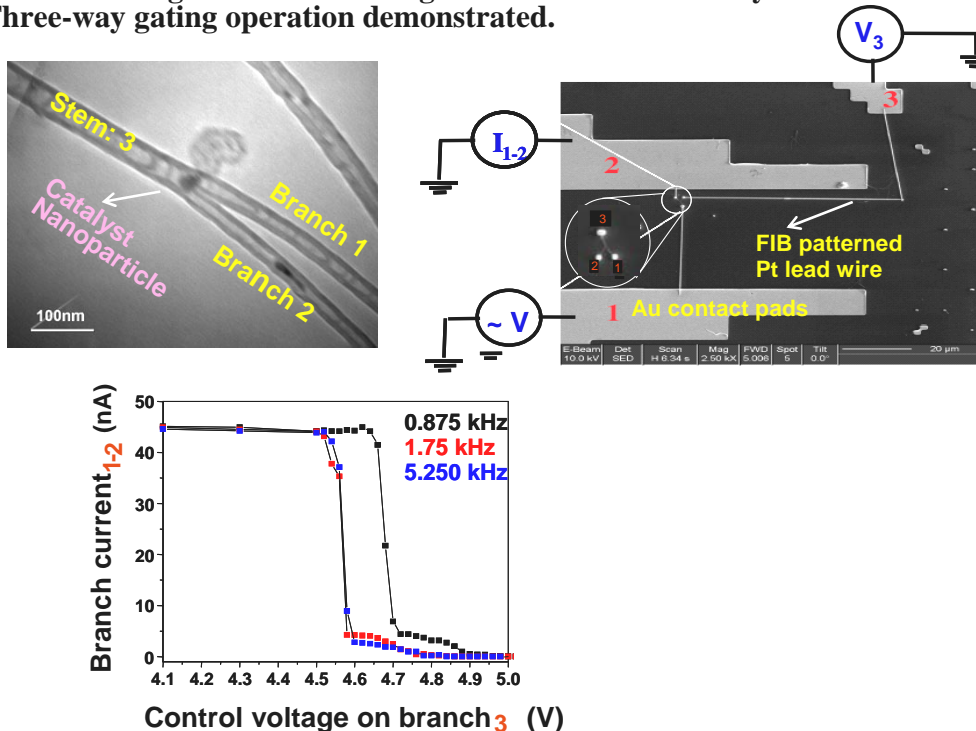
Daraio, and Sungho Jin, *Nano Lett.* **4**, 1781 (2004).

--- Joseph F. AuBuchon, Li-Han Chen, and Sungho Jin, *J. Phys. Chem. B* **109**, 6044-6048 (2005).

## Nanoelectronics

### Carbon Nanotubes for Nanoelectronics --- Electrical Switching Behavior and Logic in CNT Y-Junction Transistors

- P.R. Bandaru, C. Daraio, S. Jin, and A.M. Rao, *Nature Materials* **4**, 663 (2005).
- Sharp transistor switching behavior enabled by 3<sup>rd</sup> branch as a gate.
- Natural CNT gate – No external gate fabrication necessary.
- Three-way gating operation demonstrated.



## Nanoprobe Design and Fabrication

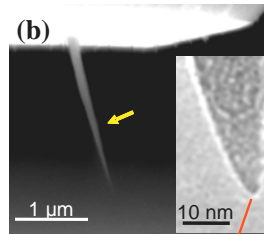
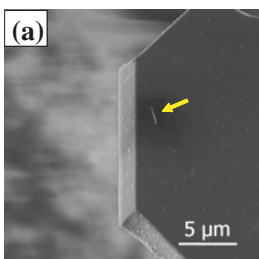
- For creation of extremely fine AFM probe tips which have desirable high-resolution and mechanical durability.
- For field emission, nano lithography applications, etc.
- Nanoscale conductance probes for biological ionic conductivity measurements near ion channels (e.g., study of Al Zheimer's disease).
- For bio engineering modification of cells with nano-needles or nano-pipettes (by insertion of genes, growth factors, drug molecules, etc.) for cell behavior study and therapeutic applications.

### Carbon Nano Cone AFM Probe on Si Cantilever

On AFM cantilever (By patterning of a single Ni island by lithography + Electric field guided chemical vapor deposition of carbon nanocones)

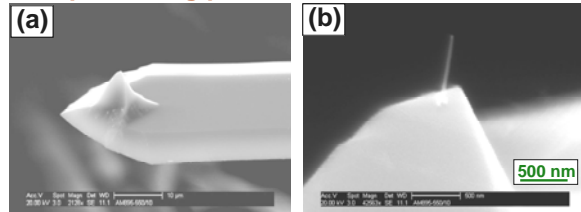
#### AFM Tips Being Made by Jin Group

- Using Sharp Carbon Nanocones.
- Tip radius of curvature ~ 1 nm regime.
- Electrically conductive (for bio imaging or conductance imaging)
- Mechanically durable.
- High aspect ratio for deep trench or via hole imaging.



~1 nm diameter tip (by TEM)

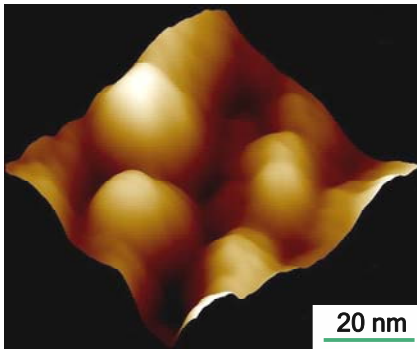
**Carbon nanocone AFM probe deposited on protruding pedestal cantilever**



### Deep Trench Imaging Capability

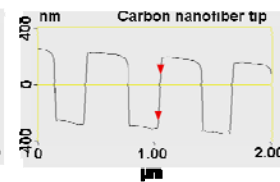
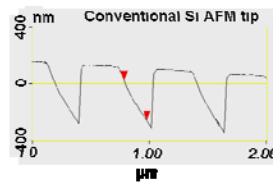
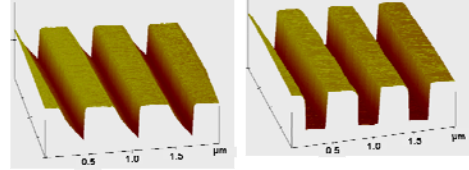
- 500 nm deep PMMA (polymethyl methacrylate) resist pattern on Si substrate, with a 300 nm line/space pattern

**High Resolution AFM Image of Cu Film by Carbon Nanocone Probe**

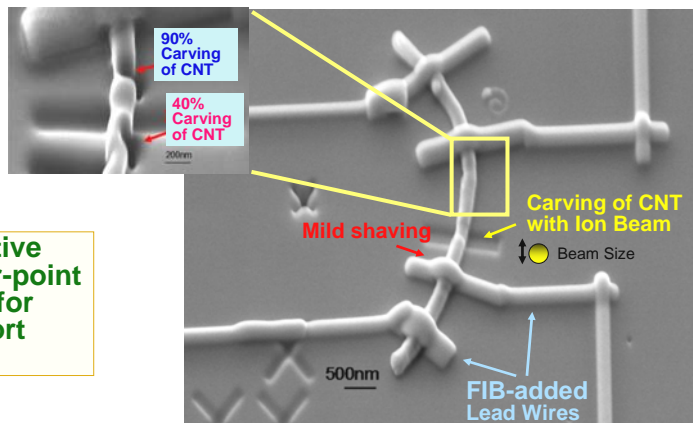


**Standard Si AFM Tip**  
(erroneous image)

**Carbon Nanocone Tip**  
(more accurate image)



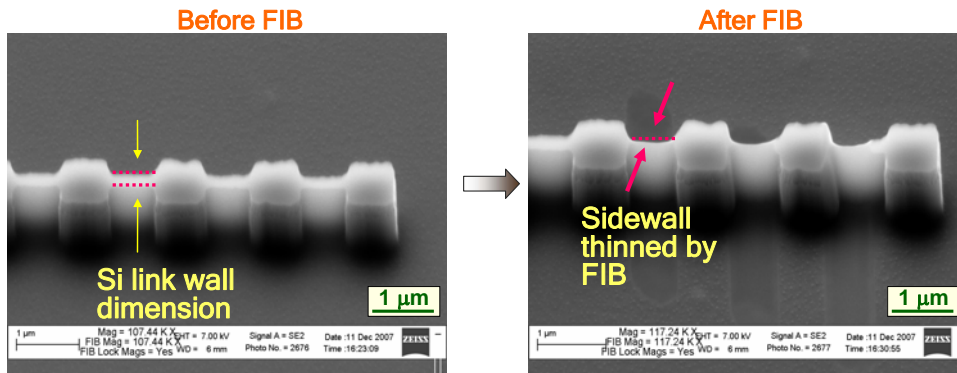
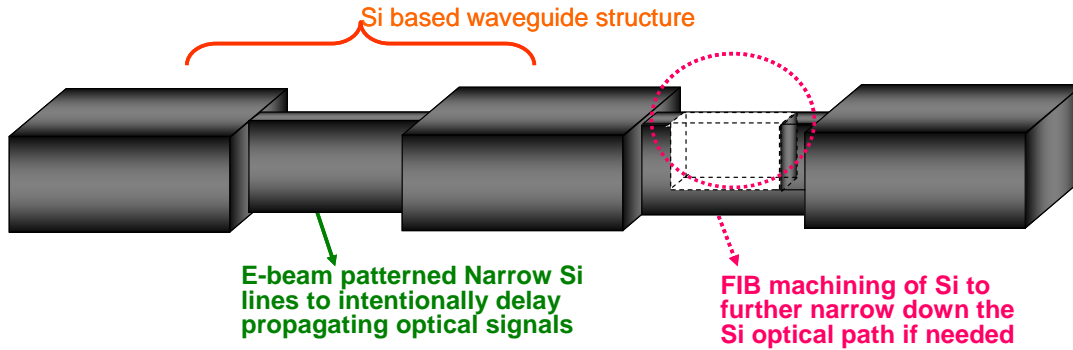
### Focused Ion Beam Modification of Nanostructures



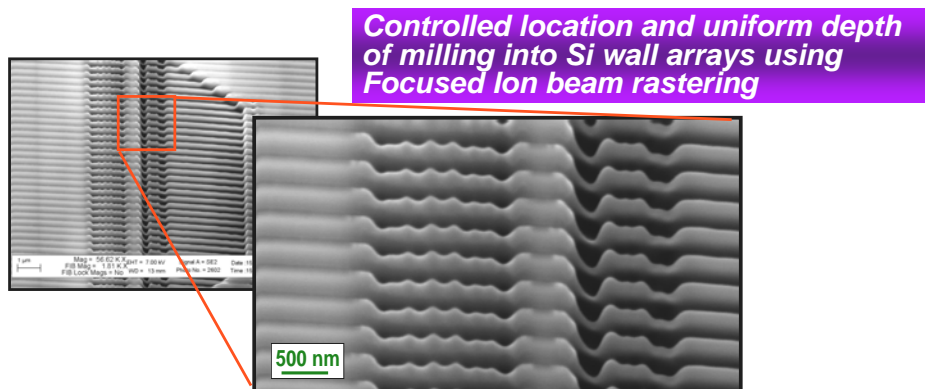
**CNT with subtractive line defects + four-point lead wires added for electronic transport measurements**

## Silicon Nano-Photonics – for future, ultra-high-density semiconductor circuits

- Focused ion beam carved to introduce delay lines for light propagation and to locally slow down light movement through Si wave guide – by fabricating smaller, dimensionally optimized paths.

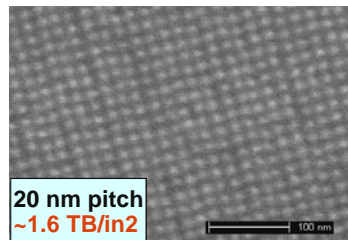
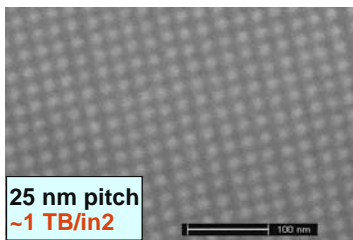
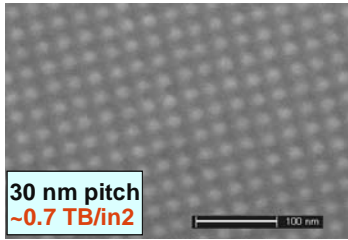
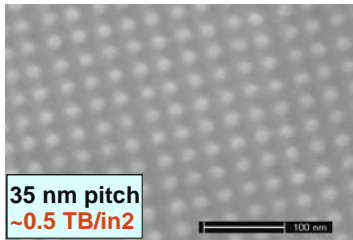


## FIB-induced geometry manipulations for thinning and necking of Si nanowire paths --- To create wavy Si, necked Si, narrowed wall Si



## Nanofabrication of 10-15 nm features

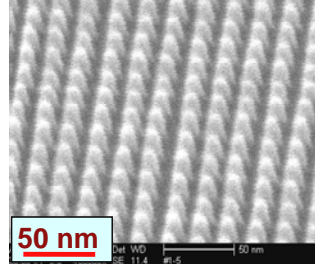
**E-beam patterned HSQ resist island array with 1.6 TB/in<sup>2</sup> density on Si.**



**Pattern transferred to Si island array with ~10 nm dia. and magnetic island deposited on pillar top**

**1.6 Terabit/in<sup>2</sup> density**

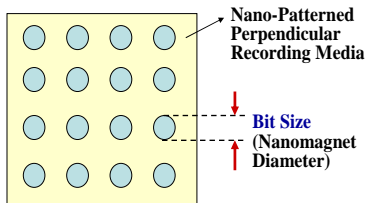
**(b) 10nm dia x 20nm height**



## Magnetic Nanostructure and Patterned Recording Media

- There is a need to substantially increase the density of magnetic recording media.
- Patterned media with periodic array of ~10-20 nm regime magnetic nanoislands or nanowire magnets are highly desirable.
- 10-20 nm nanomagnet dimension is well below the available lithography limit.
- New, innovative synthesis/fabrication approaches are desirable.

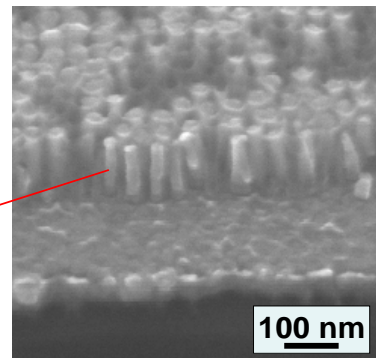
### Upper Limit Recording Density vs Bit Size



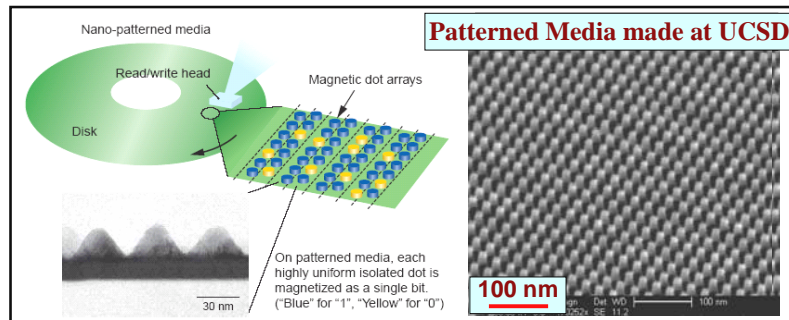
Bit Size (nm)	2	3	5	10	12.5	15	20
Period, (nm)	(4)	(6)	(10)	(20)	(25)	(30)	(40)
Recording Density (TB/in <sup>2</sup> )	42	18	6.5	1.6	1.0	0.7	0.4

**Successfully Fabricated ~20 nm Diameter Vertically aligned CoPt Nanomagnets in Anodized Aluminum Oxide Membranes**

CoPt nanomagnets (aluminum oxide matrix dissolved away to show the nanowires)



## Advanced Patterned Recording Media by Nanofabrication

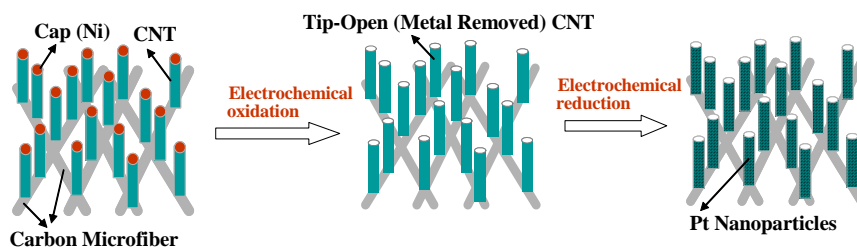


- One bit per each 'island' approach -- To go beyond the current hard disk memory limit of  $\sim 200$  GB/in<sup>2</sup> memory.
- Areal memory densities of more than **1 TB/in<sup>2</sup>** desired.
- Difficulty in 10 nm regime bit fabrications, large area, in circular periodic pattern --- very challenging.
- For eventual manufacturing for large-area patterning, *Nano-imprint Lithography* is the most viable technology.

## Energy-Related Materials

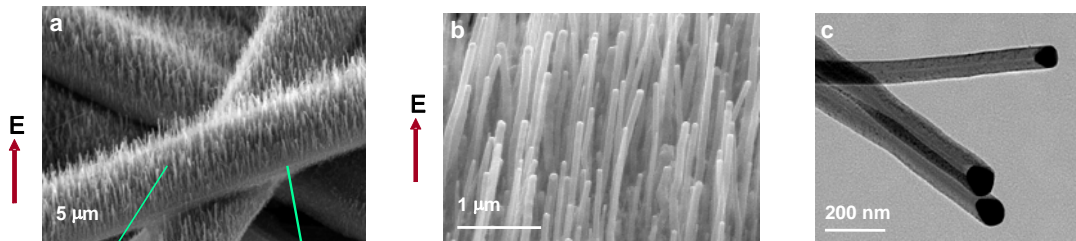
### Electrochemical Modification of Vertically Aligned Carbon Nanotube Arrays

- The presence of metal particles (e.g., Ni) may interfere with the intended chemical or electrochemical reactions.
- **Tip-Opening (oxidation) + electrodeposition of Pt nanoparticles (reduction)** onto vertically-aligned CNT arrays.



### Carbon Nanotube Array for Fuel Cell Applications

- On conductive substrate (carbon microfiber, carbon paper)
- As electrode material to carry Pt catalyst particles



Aligned and separated carbon nanotubes (30-60 nm dia)

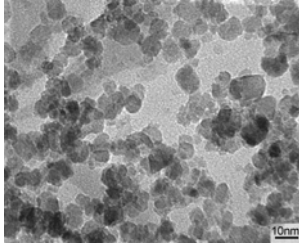
Carbon microfiber conductors ( $\sim 5 \mu\text{m}$  dia.)

## Bio Materials

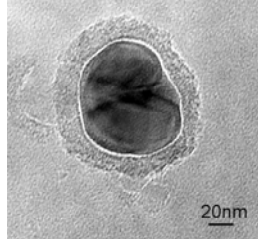
### Examples of Synthesis and Applications of Magnetic Nanoparticles

Potential Bio Applications – Cancer treatment, gene delivery, neural regeneration, drug delivery, magnetic cell sorting, MRI.

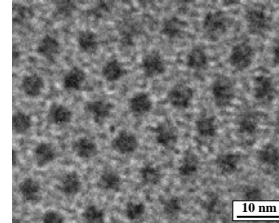
(a) Superparamagnetic  $\text{Fe}_3\text{O}_4$



(b) Silica-Coated  $\text{Fe}_3\text{O}_4$



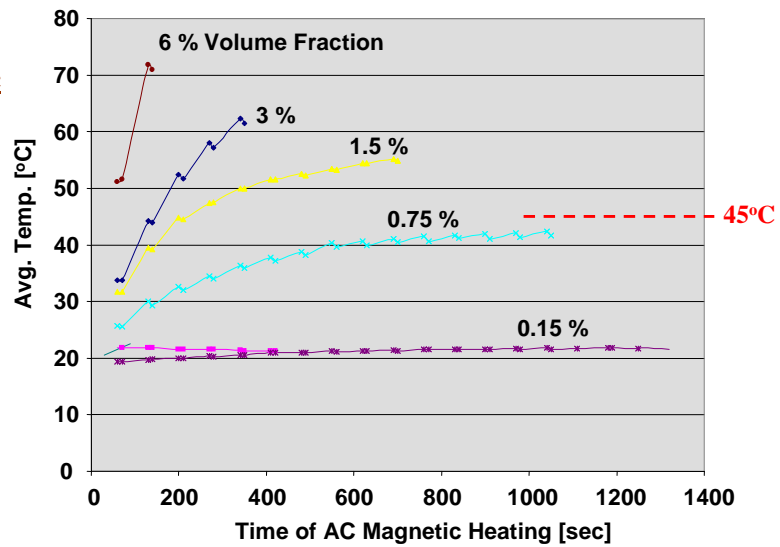
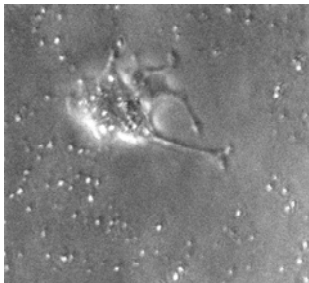
(c)  $\text{Fe}_3\text{O}_4$  Magnetic Nanoparticle Array



### Temperature rise induced by remote magnetic field (100 KHz)

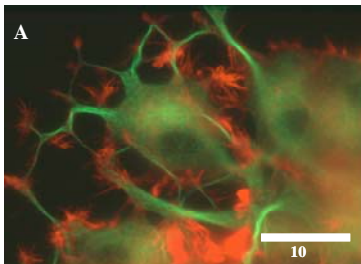
- In a liquid containing various volume of magnetic nanoparticles.
- ~10 nm diameter  $\text{Fe}_3\text{O}_4$  particles.
- Live cell magnetic hyperthermia experiments to be carried out.

**PC-12 Neural Cancer Cells with Endocytosed Magnetic Nanoparticles** -- Can be stimulated into Neurite growth by NGF growth factor

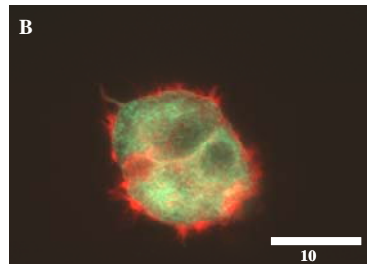


### Nanotoxicity Study --- Response of PC12 Cells to Magnetic Nanoparticles

$\text{Fe}_3\text{O}_4$  conc. = 0.15 mM



$\text{Fe}_3\text{O}_4$  conc. = 15 mM (dramatic reduction in ability to generate neurites with increased concentration of magnetic nanoparticles --- ~spherical cell shape with much decreased surface area)

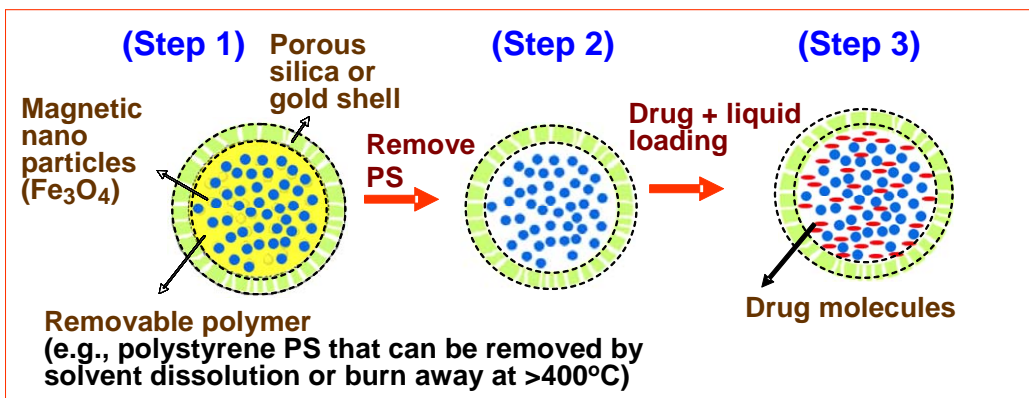


Immunofluorescence of typical PC-12 cells 4 days after endocytosis. Cytoskeletal structure shown with tubulin (fluorescein, green) and actin (rhodamine, TRITC labelled phalloidin, red).

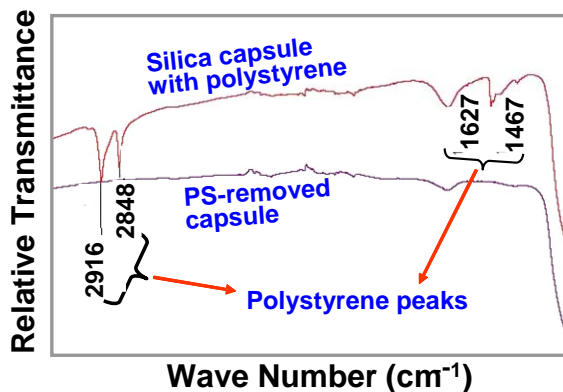
## Magnetically Guidable, Remote-Controlled Drug Delivery Nanocapsules

- Existing drug therapeutic techniques --- Inefficient in deep tumor drug delivery and lack on-demand drug release.
- A new technique that allows better drug penetration into cancer cell aggregates within tumors and subsequent switchable release is highly desirable.
- Developed hollow-sphere nanocapsules containing intentionally trapped magnetic nanoparticles and defined anticancer drugs --- To provide a powerful magnetic vector under moderate gradient magnetic fields.
- These drug-loaded nanocapsules can penetrate into the interior of tumors and allow a controlled on-off switchable release of the anticancer drug cargo via remote RF field.
- This imageable smart drug delivery system is compact (80~150 nm capsules).
- *In vitro* as well as *in vivo* results --- indicate that these nanocapsule-mediated, on-demand drug release is effective in reducing tumor cell growth.
- This magnetic vector nanotechnology may also be utilized to move the nanocapsules through BBB so as to release CNS drugs at selected locations.

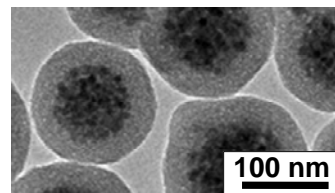
### (a) Drug-carrier nanocapsule fabrication and drug insertion



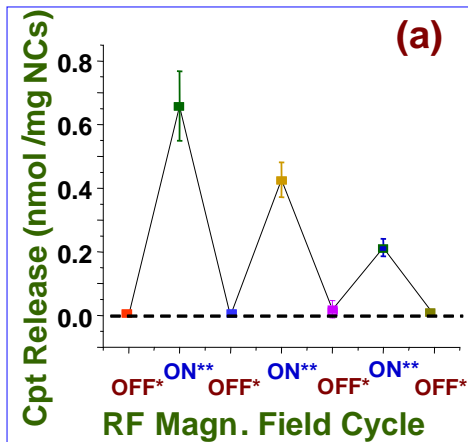
### (b) FTIR confirmed PS removal



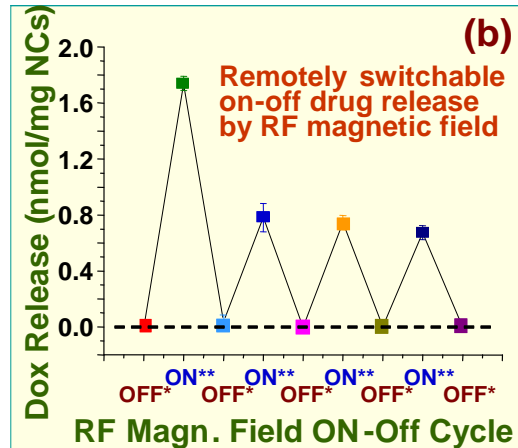
(c) TEM of nanocapsules (~100 nm) with trapped  $\text{Fe}_3\text{O}_4$  magn. nanoparticles (10 nm dia, 45 vol. %)



### Hydrophobic drug release (CPT)

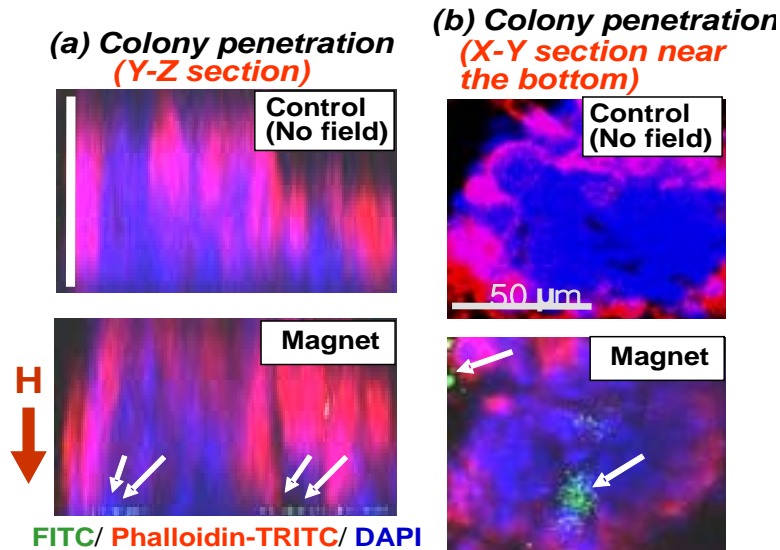


### Hydrophilic drug release (DOX)



On-off switchable release from the magnetic nanocapsules. (a) Release of hydrophobic camptothecin (nanomole per mg nanocapsule, NC) by RF magnetic field on-off cycling (switch-on period=10 seconds, switch off=5 minutes), (b) A similar switchable release is demonstrated for hydrophilic doxorubicin from the nanocapsules by RF field.

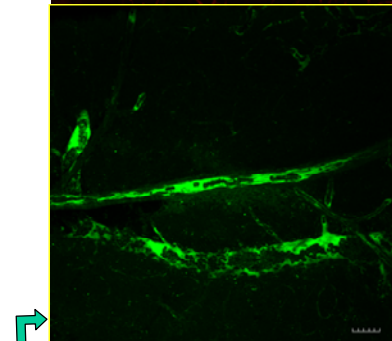
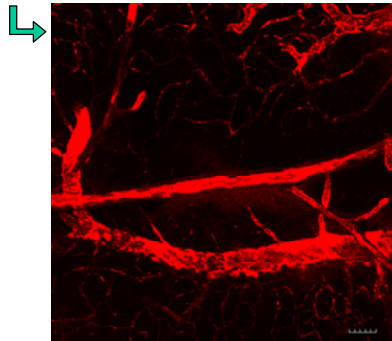
### Tissue penetration by magnetic vector



Confocal microscopy images of the magnetic nanocapsule penetration into MT2 breast cancer cell colony using magnet gradient pulling force (vertical scale bar=50  $\mu$ m) applied for 2 hrs by a Nd-Fe-B magnet ( $H \sim 1,200$  Oe near the cancer colony location). The Y-Z vertical section image, and X-Y horizontal section image near the bottom demonstrate a successful penetration of cancer colony by magnetic nanocapsules.

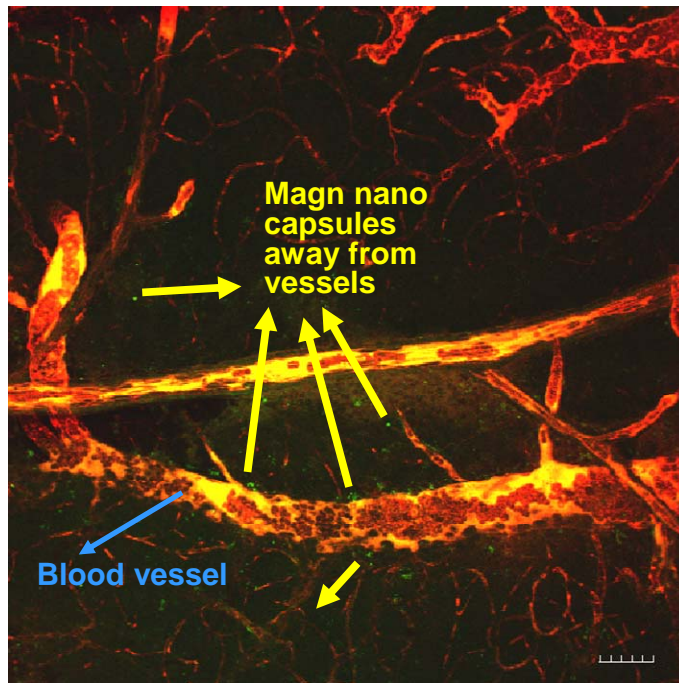
Confocal microscopy for BBB crossing [Polystyrene surface + fluorescent dye attached + tail vein injection on mouse + confocal microscopy to trace magnetic nanocapsules (green)]. – BBB crossing is observed.

Blood vessel (TRITC-dextran, red)



Anthracene-Nanoparticle (green)

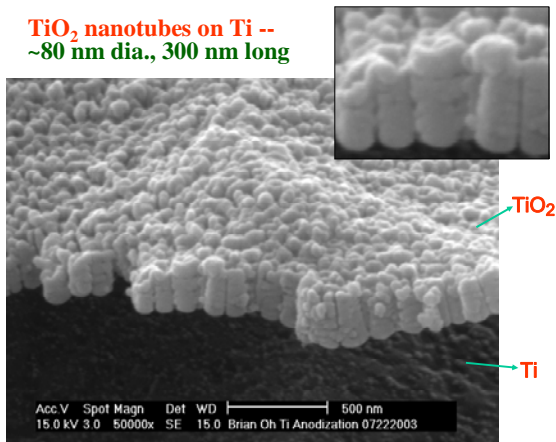
Red and green merged image



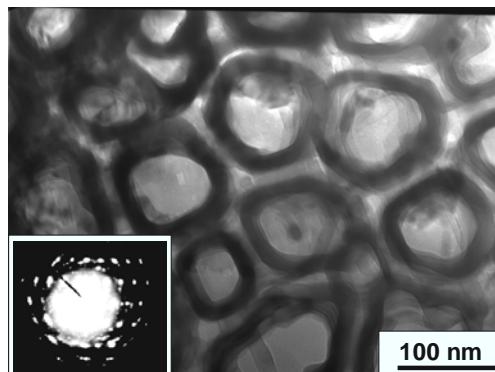
Scale bar = 50um

### Effect of Nanostructure of Bio Materials on Cell Growth

TiO<sub>2</sub> nanotubes on Ti --  
~80 nm dia., 300 nm long

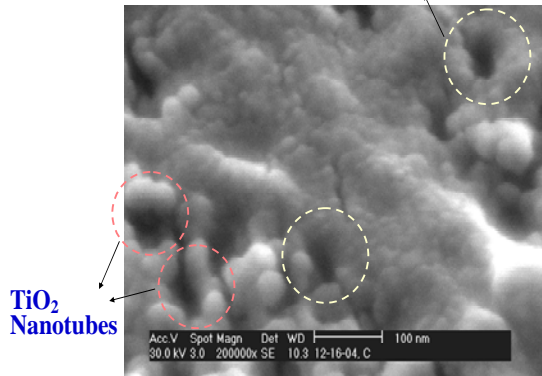


Top View TEM Micrograph of Aligned TiO<sub>2</sub> Nanotubes

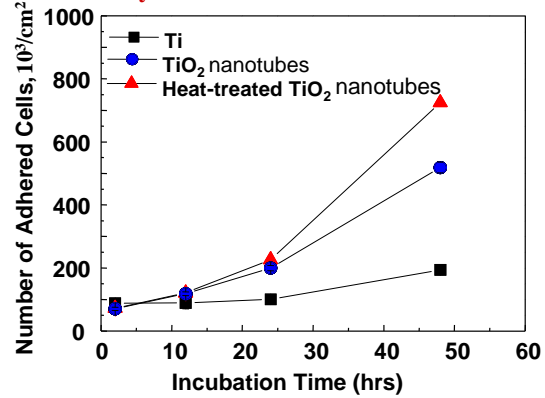


**Enhanced Osteoblast Cell Adhesion and Lock-In on Anatase TiO<sub>2</sub> Nanotubes**

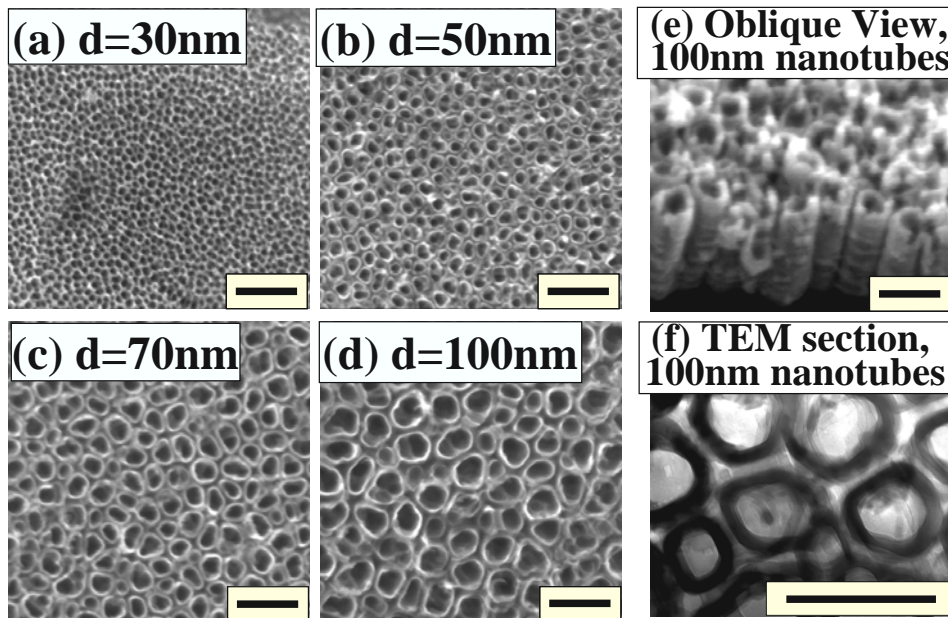
**Cell Growth into TiO<sub>2</sub> Nanotubes**



**Effect of TiO<sub>2</sub> Nanotube Layer on Osteoblast Cell Growth --- Significantly Accelerated Growth by ~ 300 – 400%**



**Control of Stem Cell Differentiation Dictated Soly by Nanotube Dimension**



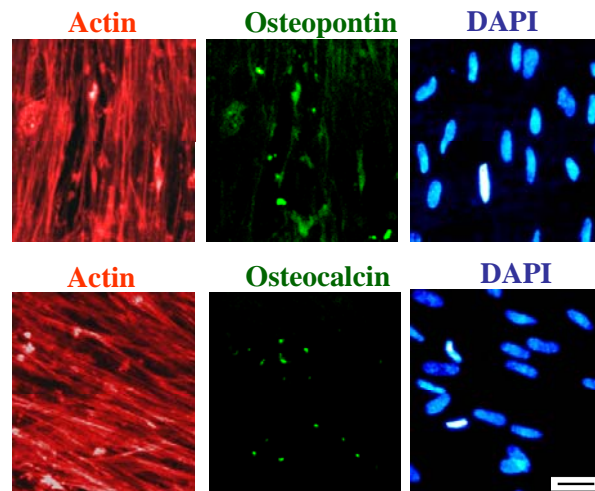
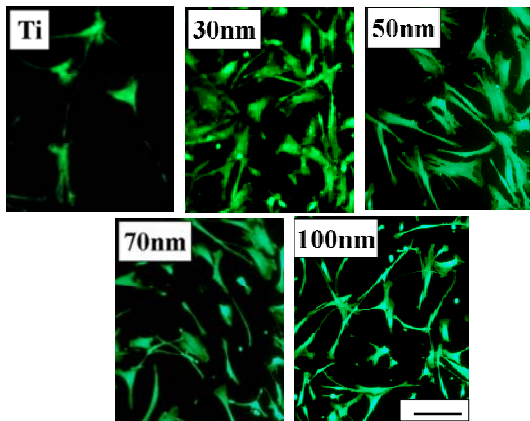
SEM micrographs of self-aligned TiO<sub>2</sub> nanotubes with significantly different diameters. The self-assembly layers were generated by anodizing Ti sheets. The images show highly ordered, vertically aligned nanotubes with four different nanotube pore diameters between approximately 30-100nm, created by controlling potentials ranging from 5 to 20 V. (e) Right-Top image is the oblique view of the 100 nm diameter TiO<sub>2</sub> nanotube, and (f) right-bottom image is the cross-sectional transmission electron microscopy (TEM) of the 100 nm dia. TiO<sub>2</sub> nanotubes. (All scale bars: 200 nm)

## Effect of Nanostructured Substrate on Growth of Mesenchymal Stem Cell



Immunofluorescent images of reacted stem cells on 100nm diameter TiO<sub>2</sub> nanotubes after 3 weeks of culture. (Scale bar: 50  $\mu$ m)

FDA images of hMSCs on flat Ti and various diameter TiO<sub>2</sub> nanotubes (24 hr culture, Scale bar=100  $\mu$ m).



- TiO<sub>2</sub> nanotube dimension significantly influences the hMSC (human mesenchymal stem cell) differentiation behavior
- Smaller diameter nanotubes (~30 nm dia) enhance cell adhesion and proliferation without differentiation, while larger diameter nanotubes (~100 nm dia) cause the stem cells to substantially elongate, stressed and preferentially differentiate into bone cells (osteoblasts), which can be useful for orthopaedic and dental applications.

- Seunghan Oh, Karla Brammer, Julie Li, Dayu Teng, Adam Engler, Shu Chien, Sungho Jin, “Stem Cell Fate Dictated Solely by Altered Nanotube Dimension”, *PNAS* 106(7), 2130-2135 (2009).
-